ADVANCED FUNCTIONAL MATERIALS

Supporting Information

for *Adv. Funct. Mater.*, DOI: 10.1002/adfm.201904278

Strong Electronic Interaction of Amorphous Fe_2O_3 Nanosheets with Single-Atom Pt toward Enhanced Carbon Monoxide Oxidation

*Wenlong Chen, Yanling Ma, Fan Li, Lei Pan, Wenpei Gao, Qian Xiang, Wen Shang, Chengyi Song, Peng Tao, Hong Zhu, Xiaoqing Pan, Tao Deng, and Jianbo Wu**

Supporting Information

Strong electronic interaction of amorphous Fe_2O_3 nanosheets with single atom Pt towards enhanced carbon monoxide oxidation

*Wenlong Chen, Yanling Ma, Fan Li, Lei Pan, Wenpei Gao, Qian Xiang, Wen Shang, Chengyi Song, Peng Tao, Hong Zhu, Xiaoqing Pan, Tao Deng and Jianbo Wu**

Calculation section

S1.1 Binding Energy Analysis

Binding energy analysis on Pt-SA/A-Fe_2O_3, Pt-SC/A-Fe_2O_3, and Pt-SN/A-Fe_2O_3, provides valuable information on how Pt interacts with the support. The binding energy, E_{BE}, between Pt-SA/A-Fe_2O_3, Pt-SC/A-Fe_2O_3, and Pt-SN/A-Fe_2O_3 can be defined as:

$$E_{BE} = (E_{tot} - E_{Pt} - E_{sub})/N$$

Where E_{tot} is the energy of the total energy of Pt-SA/A-Fe_2O_3, Pt-SC/A-Fe_2O_3, and Pt-SN/A-Fe_2O_3, E_{Pt} is the energy of Pt in different size, E_{sub} is the energy of the Fe2O3 A support and N is the number of Pt atoms.

S1.2 Charge Density Difference

To explore the electron behavior between Pt and support, charge density difference was defined as follows:

$$\Delta\rho_{AB} = \rho_{AB} - \rho_A - \rho_B$$

where $\Delta\rho_{AB}$ is the charge density difference, ρ_{AB}, ρ_A and ρ_B is charge density of total slab, the corresponding Pt in various size and the support slab, respectively.

S1.3 Bader Charge Analysis

To gain more accurate insight into electronic interaction at the interface between Pt and the support, we calculated the charge accumulation direction using the Bader charge analysis.[5-8] The transfer electron mainly including average, maximum and minimum extra electrons were shown in Table S3.

S1.4 Adsorption Energy

Adsorption energy for CO and O2 on four configurations including A-Fe_2O_3 Pt-SA/A-Fe_2O_3, Pt-SC/A-Fe_2O_3, and Pt-SN/A-Fe_2O_3, are determined (Figure 3a). The definition of adsorption energy is similar to our previous work.[9]

S1.5 The d Band Center Analysis

We also calculated the d-band center of Pt atoms in slab using the following formula:

$$\varepsilon_{\mathrm{d}} = \frac{\int_{-\infty}^{+\infty} n_d(\varepsilon)\varepsilon d\varepsilon}{\int_{-\infty}^{+\infty} n_d(\varepsilon) d\varepsilon}$$

where ε_{d} is the d band center with respect to Fermi level, $n_d(\varepsilon)$ is the density of states about d band and ε represents the energy.

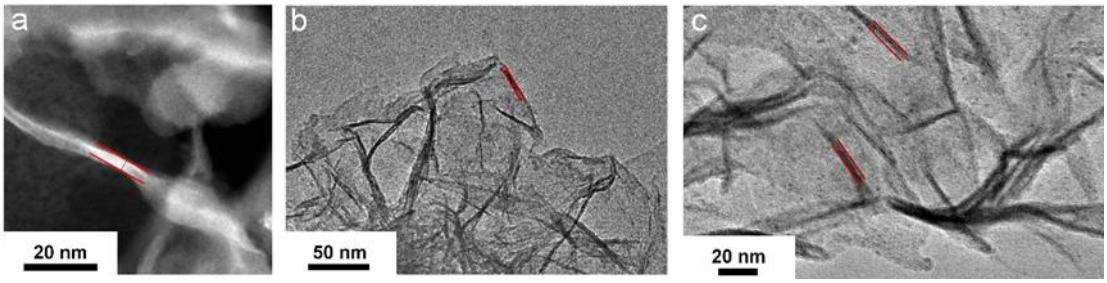

Figure S1. High magnification of the nanosheets side view with (a) HAADF-STEM and (b, c) HRTEM for typical as-prepared nanocatalysts. Thickness measured from the nanosheets side in the images. (a) ~3.2nm, (b) average ~3.0nm, (c) average ~3.2nm.

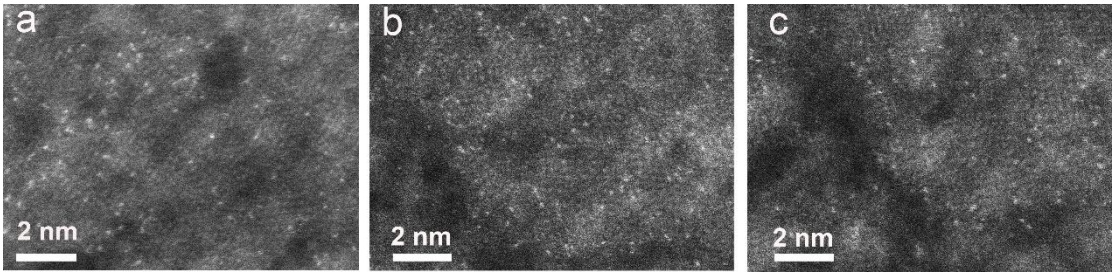

Figure S2. More HAADF-STEM images for Pt-SA/A-Fe_2O_3 catalyst, indicating the atomically dispersed Pt.

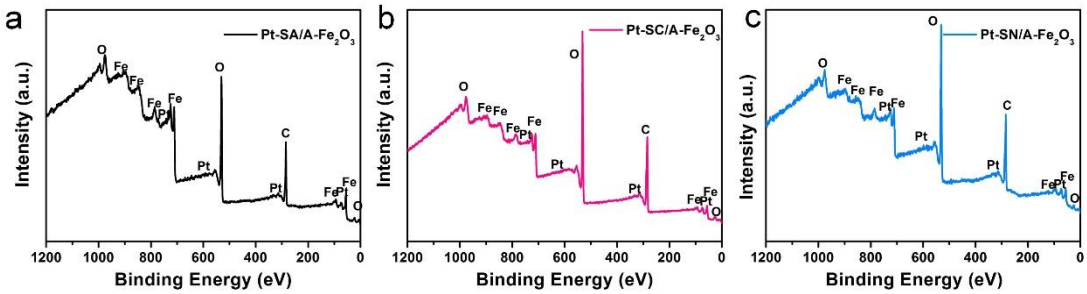

Figure S3. Full XPS spectrum with all elements and peaks for the related samples.

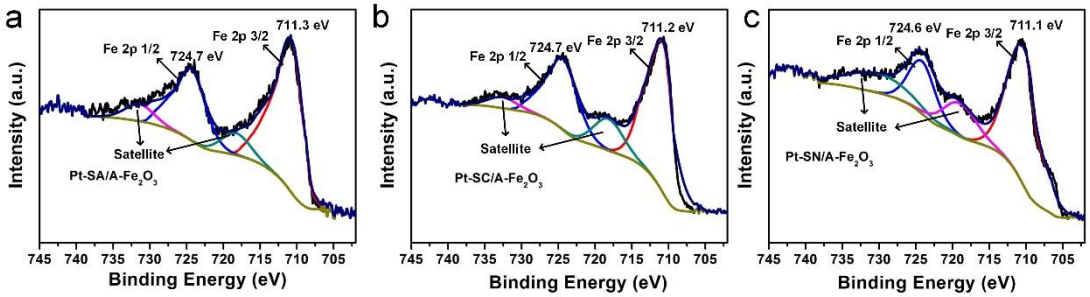

Figure S4. XPS with deconvoluted peaks of as-prepared Pt-SA/A-Fe_2O_3, Pt-SC/A-Fe_2O_3, and Pt-SN/A-Fe_2O_3.

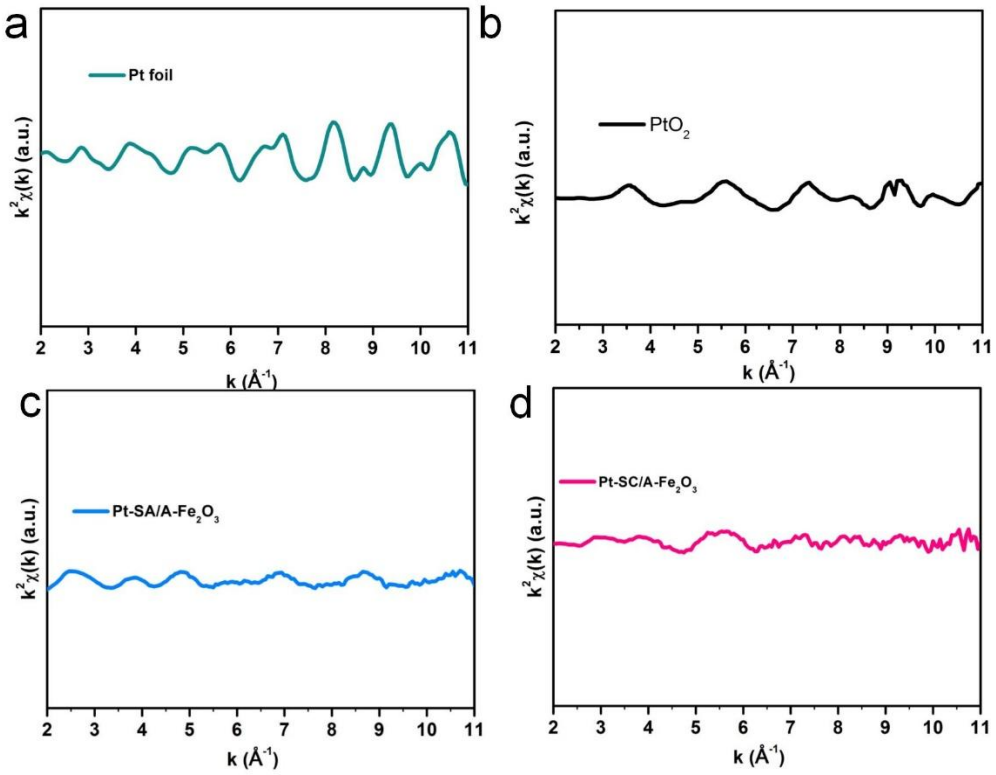

Figure S5. EXAFS χ(k) signals in k-space for the different samples.

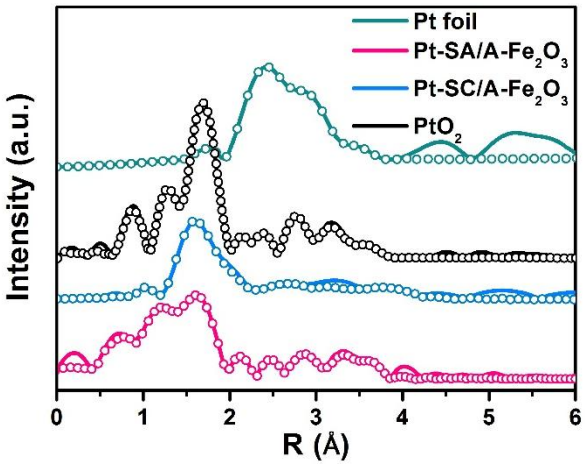

Figure S6. The Pt Fourier transform-EXAFS spectrum in R space for various samples. The circles scatter lines are the corresponding fitted curves.

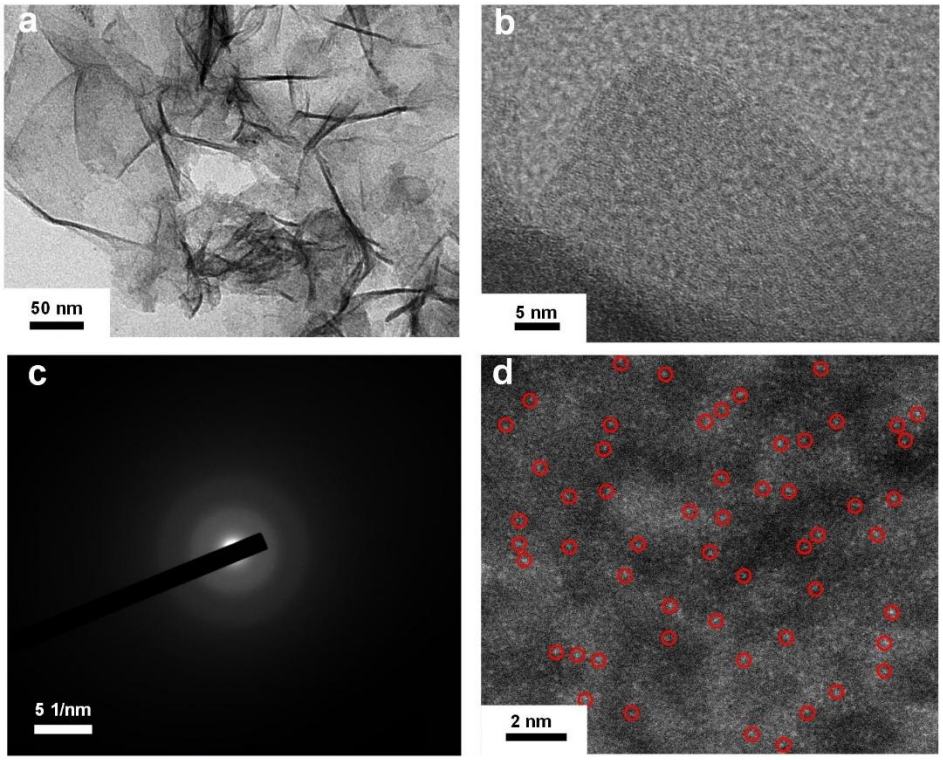

Figure S7. Structural characterizations of (a) Low-magnification TEM image, (b) HRTEM (c) SAED and (d) HAADF-STEM image for Pt-SA/A-Fe_2O_3 catalyst after CO oxidation stability test.

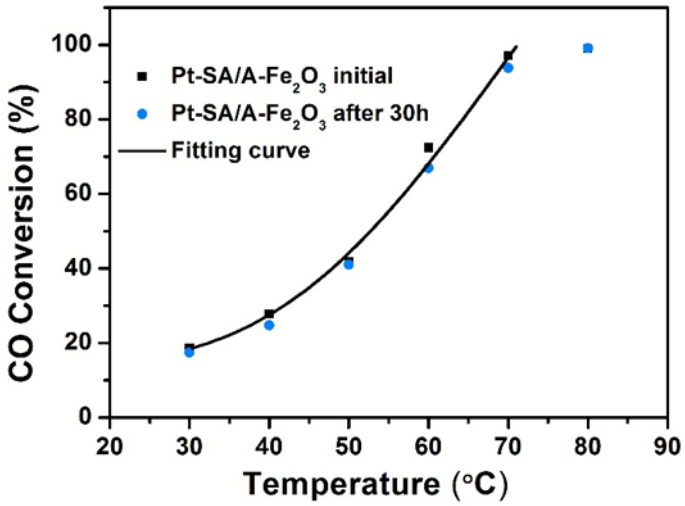

Figure S8. Comparison of the CO conversion performance for the Pt-SA/A-Fe_2O_3 catalyst in 0h and after 30h use.

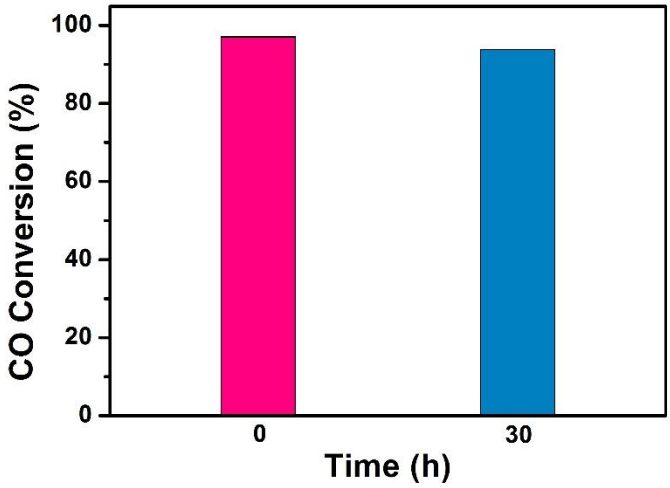

Figure S9. Comparison of the CO conversion performance at 70 ℃ for the Pt-SA/A-Fe_2O_3 catalyst in 0h and after 30h use.

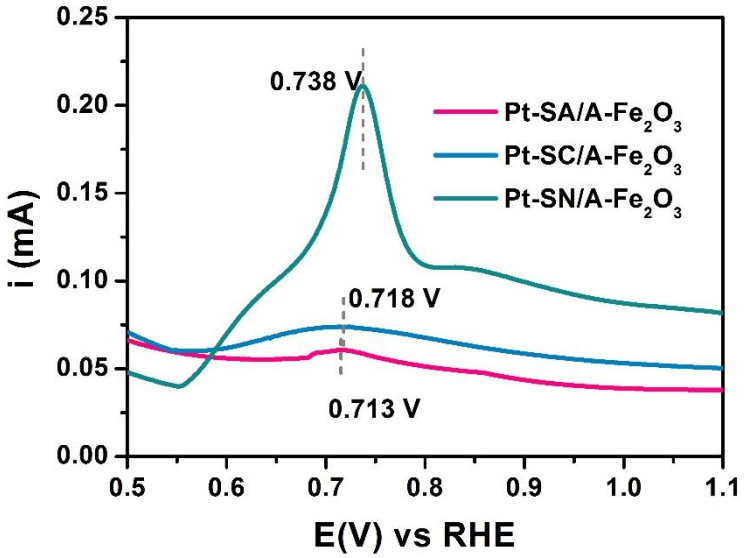

Figure S10. CO stripping voltammograms of various catalysts with the same Pt mass loading.

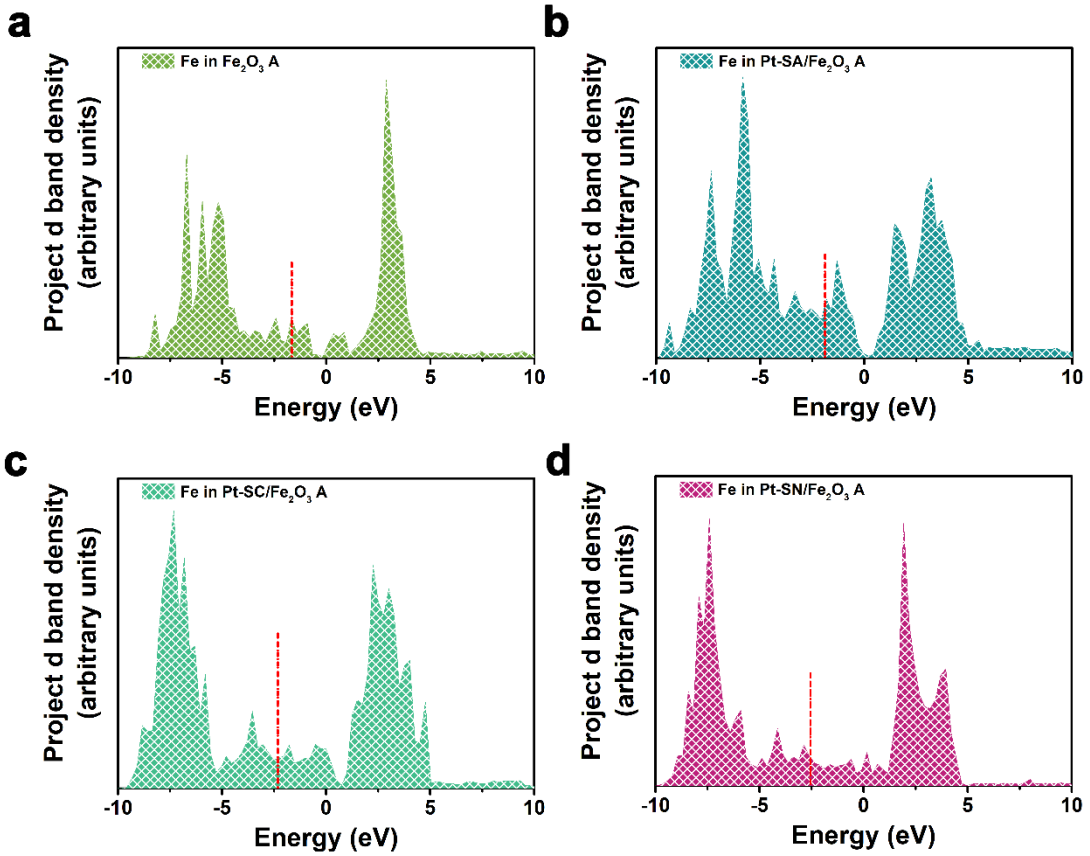

Figure S11. Projected d band density of (a) Fe in A-Fe_2O_3, (b) Fe in Pt-SA/A-Fe_2O_3, (c) Fe in Pt-SC/A-Fe_2O_3, (d) Fe in Pt-SN/A-Fe_2O_3. The red line in projected d band density indicates the corresponding d band center.

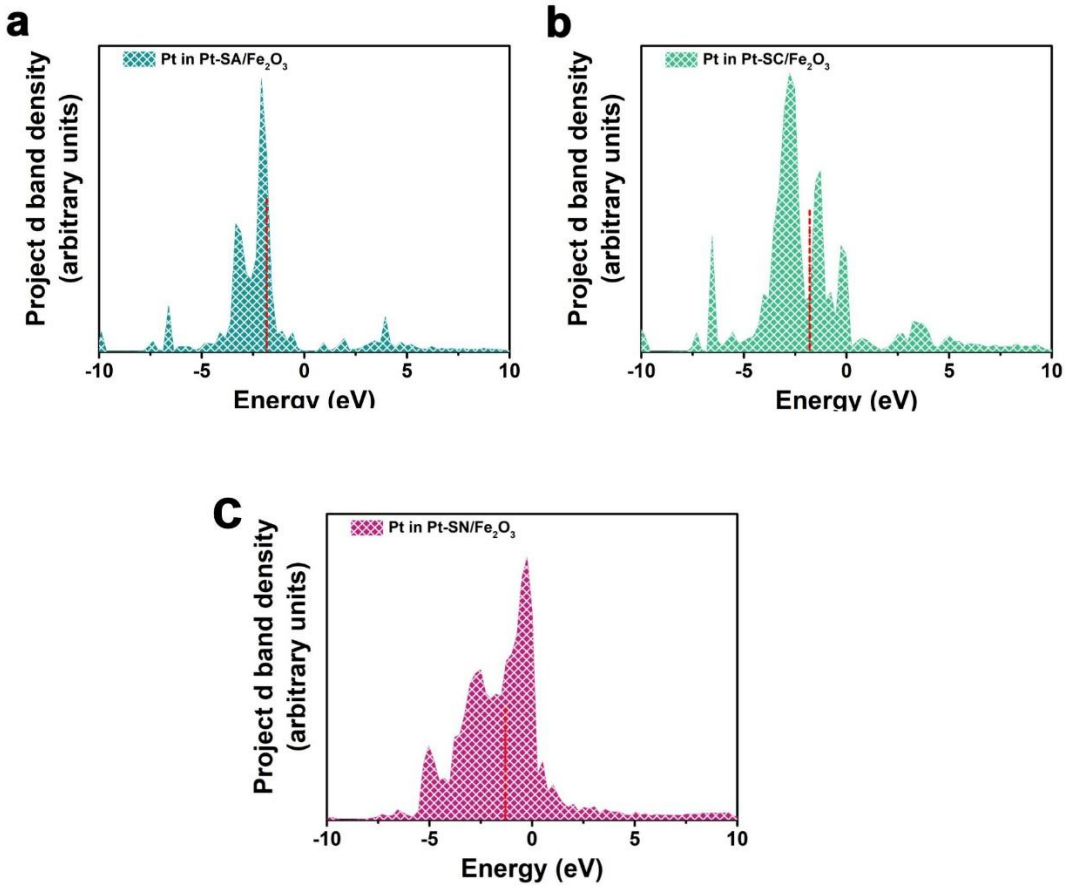

Figure S12. Projected d band density of (a) Pt in Pt-SA/ A-Fe_2O_3, (b) Pt in Pt-SC/ A-Fe_2O_3, (c) Pt in Pt-SN/ A-Fe_2O_3. The red line in projected d band density indicates the corresponding d band center.

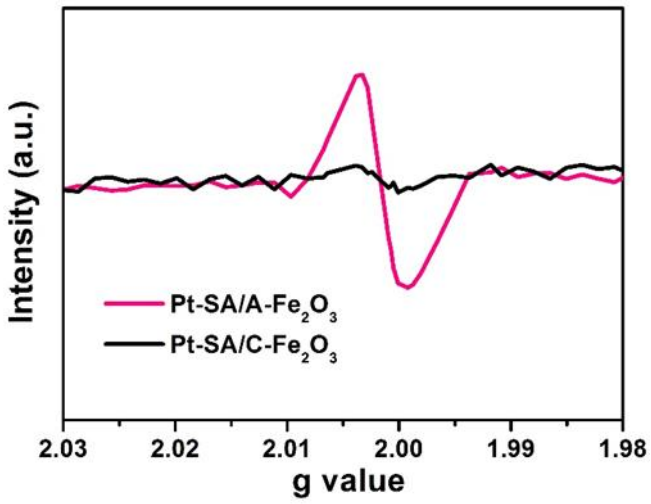

Figure S13. EPR of Pt-SA/A-Fe_2O_3 and Pt-SA/C-Fe_2O_3 samples.

Table S1. ICP results of different Pt/A-Fe_2O_3 catalysts.

catalysts	Pt ratio (wt.%)
Pt-SA/A-Fe_2O_3	1.20%
Pt-SC/A-Fe_2O_3	4.56%
Pt-SN/A-Fe_2O_3	8.62%

Table S2. EXAFS fitting parameters of samples

sample	shell	*N*	R (Å)	$\Delta\sigma^2$ (Å2)
Pt foil	Pt-Pt	12.0	2.75	0.005
PtO_2	Pt-O	6.0	2.02	0.003
	Pt-Pt	6.0	3.02	0.002
Pt-SA/A-Fe_2O_3	Pt-O	4.1	2.00	0.005
	Pt-Fe	1.2	2.57	0.003
Pt-SC/A-Fe_2O_3	Pt-O	2.0	1.98	0.003
	Pt-Pt	2.1	2.77	0.007
	Pt-Fe	1.0	2.53	0.005

Note: *N*, R and σ2 are the coordination number, the average distance between absorber and backscatter atoms, Debye−Waller factor

Table S3. comparisons of the CO oxidation performance with references

samples	Metal loadings (wt%)	Temperature (℃)	specific rate × 10^2, mol_{CO} h^{-1} g_{Pt}^{-1}	TOF × 10^2, s^{-1}	note
Pt-SA/A-Fe_2O_3	1.2	70	125.0	6.87	This work
Pt-SA/C-Fe_2O_3	1.2	70	81.6	4.4	This work
Pt1/FeOx	0.17	27	43.5	13.6	Nature chemistry, 2011, 3(8): 634.
Au/Fe_2O_3	4.4	27	39.3	8.6	ACS Catal. 2014, 4, 2113−2117
Pt/Al_2O_3	2.0	80	--	~0.2	Chem. Commun. 2005, 1429−1431.
Pt/Fe_2O_3	5.11	60	71.1	2.40	ACS applied materials & interfaces 2018,10 (17), 15322-15327
0.18% Pt/θ-Al_2O_3	0.18	200	-	1.3	J. Am. Chem. Soc. 2013, 135, 12634−12645
Ir1/FeOx	0.01	300	43.4	2.31	J. Am. Chem. Soc. 2013, 135, 15314−15317
Pt/γ -Al_2O_3		150		1.1	J. Chem. Tech. Biotechnol. 52, 415 (1991)
Ir/TiO_2	5.0	350	12	2.9	Appl. Catal., A 1996, 139, 131

Table S4. Bader charge of Pt on the surface of Pt-SA/A-Fe_2O_3, Pt-SC/A-Fe_2O_3 and Pt-SN/A-Fe_2O_3.

System	Average extra electron towards Pt atoms (e^-)	Maximum extra electron towards Pt atom (e^-)	Minimum extra electron towards Pt atom (e^-)
Pt-SA/A-Fe_2O_3	+0.746	+0.746	+0.746
Pt-SC/A-Fe_2O_3	+0.221	+0.370	-0.018
Pt-SN/A-Fe_2O_3	+0.114	+0.269	-0.058

Table S5. Binding energy between Pt-SA/A-Fe_2O_3, Pt-SC/A-Fe_2O_3 and Pt-SN/A-Fe_2O_3.

System	Binding energy (eV/atom)
Pt-SA/A-Fe_2O_3	-10.483
Pt-SC/A-Fe_2O_3	-5.317
Pt-SN/A-Fe_2O_3	-2.457

Table S6. The stable adsorption energy of CO and O_2 for Pt-SA/A-Fe_2O_3, Pt-SC/A-Fe_2O_3 and Pt-SN/A-Fe_2O_3

System	E_{CO_ads} (eV)	E_{O2_ads} (eV)
Pt-SA/A-Fe_2O_3	-2.218	-0.966
Pt-SC/A-Fe_2O_3	-2.252	-0.424
Pt-SN/A-Fe_2O_3	-2.767	-0.272

Table S7. The d-band center (relative to the Fermi level) of Pt-SA/A-Fe_2O_3, Pt-SC/A-Fe_2O_3 and Pt-SN/A-Fe_2O_3.

System	The d-band center of Pt (eV)	The d-band center of Fe (eV)
A-Fe_2O_3	/	-1.658
Pt-SA/A-Fe_2O_3	-1.830	-1.886
Pt-SC/A-Fe_2O_3	-1.797	-2.321
Pt-SN/A-Fe_2O_3	-1.304	-2.553